AD-A118 863 PRINCETON UNIV NJ DEPT OF MECHANICAL AND AEROSPACE --ETC F/G 20/4
AN EXPERIMENTAL INVESTIGATION OF THE UNSTEADY BEHAVIOR OF BLUNT--ETC(U)
MAY 82 D S DOLLING, S M BOGDONOFF N60921-81-K-0007
UNCLASSIFIED MAE-1562 NL

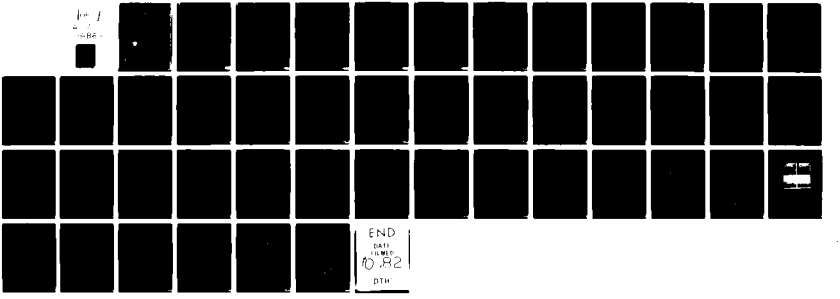

12

Princeton University

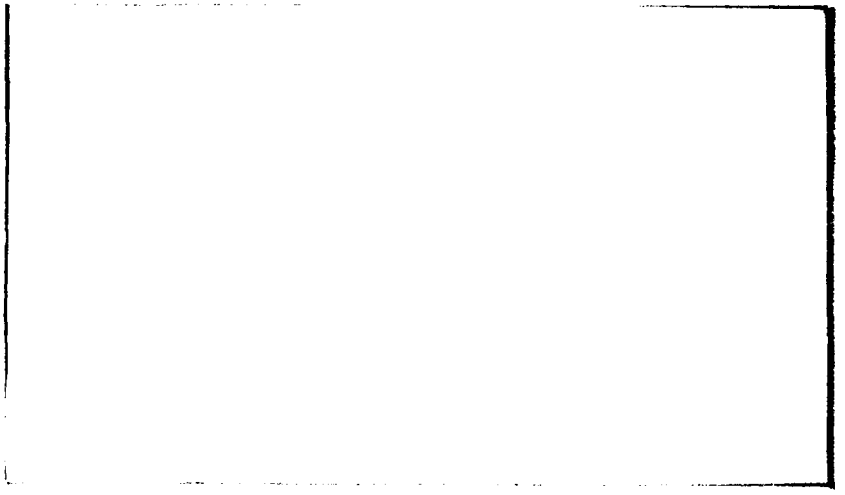

Department of Mechanical and Aerospace Engineering

AN EXPERIMENTAL INVESTIGATION OF THE UNSTEADY BEHAVIOR OF BLUNT FIN-INDUCED SHOCK WAVE TURBULENT BOUNDARY LAYER INTERACTIONS

David S. Dolling
Seymour M. Bogdonoff

Final Technical Report
Contract N60921-81-K-0007

Covering the Period 11/21/80-12/31/81

Princeton University
Report 1562-MAE

May 1982

SECURITY CLASSIFICATION OF THIS PAGE (When Data Entered)

REPORT DOCUMENTATION PAGE		READ INSTRUCTIONS BEFORE COMPLETING FORM
1. REPORT NUMBER 1562-MAE	2. GOVT ACCESSION NO. AD-A118863	3. RECIPIENT'S CATALOG NUMBER
4. TITLE (and Subtitle) AN EXPERIMENTAL INVESTIGATION OF THE UNSTEADY BEHAVIOR OF BLUNT FIN-INDUCED SHOCK WAVE TURBULENT BOUNDARY LAYER INTERACTIONS		5. TYPE OF REPORT & PERIOD COVERED Final Tech. Report 11/21/80 - 12/31/81 6. PERFORMING ORG. REPORT NUMBER
7. AUTHOR(s) David S. Dolling Seymour M. Bogdonoff		8. CONTRACT OR GRANT NUMBER(s) N60921-81-K-0007
9. PERFORMING ORGANIZATION NAME AND ADDRESS Princeton University Gas Dynamics Laboratory Forrestal Campus, Princeton, NJ 08544		10. PROGRAM ELEMENT, PROJECT, TASK AREA & WORK UNIT NUMBERS
11. CONTROLLING OFFICE NAME AND ADDRESS Naval Surface Weapons Center White Oak, Silver Spring, MD 20910		12. REPORT DATE May 1982 13. NUMBER OF PAGES 42
14. MONITORING AGENCY NAME & ADDRESS(if different from Controlling Office) Naval Air Systems Command Department of the Navy Washington, D. C. 20361		15. SECURITY CLASS. (of this report) Unclassified 15a. DECLASSIFICATION/DOWNGRADING SCHEDULE

16. DISTRIBUTION STATEMENT (of this Report)

Approved for public release; distribution unlimited

17. DISTRIBUTION STATEMENT (of the abstract entered in Block 20, if different from Report)

18. SUPPLEMENTARY NOTES

19. KEY WORDS (Continue on reverse side if necessary and identify by block number)

Three-dimensional shock wave-boundary layer interaction
Blunted fin-induced interaction
Turbulent boundary layer
Unsteady flows

20. ABSTRACT (Continue on reverse side if necessary and identify by block number)

An experimental study has been made of blunt fin-induced shock wave turbulent boundary layer interactions. This type of interaction is known to be highly unsteady. The objective of this experiment was to determine the characteristics of the fluctuating surface pressure distribution and the parameters controlling it. Tests have been made using fins of different diameter, D, with incoming turbulent boundary layers varying in thickness, δ, in the ratio of about 5:1. Measurements have been made on the fin centerline

DD FORM 1 JAN 73 1473 EDITION OF 1 NOV 65 IS OBSOLETE

Unclassified

SECURITY CLASSIFICATION OF THIS PAGE (When Data Entered)

and up to four diameters outboard of it. All tests were made at a Mach number of 2.95 and a unit Reynolds number of 6.3×10^7 m^{-1}, and under approximately adiabatic wall conditions.

The measurements show that very high intensity r.m.s. pressure levels occur — up to almost two orders of magnitude above that of the incoming boundary layer. The highest intensities occur on centerline ahead of the fin. Here, the r.m.s. pressure distribution is characterized by three distinct peaks which decrease at different rates with distance outboard. Even four diameters off centerline, the maximum r.m.s. value in the distribution is still an order of magnitude larger than that of the incoming boundary layer. Outboard of the centerline, the r.m.s. pressure level downstream of the free-stream shock wave steadily decreases. Within a distance of six to eight diameters it is close to the undisturbed value. With different diameter fins and different boundary layers, the qualitative characteristics are the same. The quantitative results depend on the ratio D/δ.

SUMMARY

An experimental study has been made of blunt fin-induced shock wave turbulent boundary layer interactions. This type of interaction is known to be highly unsteady. The objective of this experiment was to determine the characteristics of the fluctuating surface pressure distribution and the parameters controlling it. Tests have been made using fins of different diameter, D, with incoming turbulent boundary layers varying in thickness, δ, in the ratio of about 5:1. Measurements have been made on the fin centerline and up to four diameters outboard of it. All tests were made at a Mach number of 2.95 and a unit Reynolds number of 6.3×10^7 m^{-1}, and under approximately adiabatic wall conditions.

The measurements show that very high intensity r.m.s. pressure levels occur — up to almost two orders of magnitude above that of the incoming boundary layer. The highest intensities occur on centerline ahead of the fin. Here, the r.m.s. pressure distribution is characterized by three distinct peaks which decrease at different rates with distance outboard. Even four diameters off centerline, the maximum r.m.s. value in the distribution is still an order of magnitude larger than that of the incoming boundary layer. Outboard of the centerline, the r.m.s. pressure level downstream of the freestream shock wave steadily decreases. Within a distance of six to eight diameters it is close to the undisturbed value. With different diameter fins and different boundary layers, the qualitative characteristics are the same. The quantitative results depend on the ratio D/δ.

TABLE OF CONTENTS

LIST OF FIGURES

NOMENCLATURE

D	fin leading edge diameter
d	transducer sensing element diameter
M	Mach number
P	pressure
$\hat{p}$	power axis of spectral density plot (Fig. 3)
q	dynamic pressure
Re_δ	Reynolds number based on boundary layer thickness
t	time
U	velocity
u_τ	friction velocity
X	coordinate parallel to tunnel axis measured from the fin leading edge (Fig. 1)
X_s	distance parallel to X axis measured from the undisturbed freestream shock wave position (Fig. 1)
Y	coordinate normal to the X axis in the plane of the test surface measured from the fin leading edge (Fig. 1)
β	oil streak angle measured relative to undisturbed stream direction = BETA
δ	boundary layer velocity thickness
δ^*	boundary layer displacement thickness
θ	boundary layer momentum deficit thickness
ν	kinematic viscosity
τ_w	wall shear stress
ω	angular frequency, rad/sec

Subscripts and other notation

w	wall
∞	undisturbed freestream value
$< >$	r.m.s. value

1. INTRODUCTION

Over the last few years, the Gas Dynamics Laboratory at Princeton University has been carrying out experimental studies of shock wave turbulent boundary layer interactions. Several different model geometries have been used, ranging from swept[1,2] and unswept[3-7] compression corners to sharp[8-10] and hemi-cylindrically blunted fins.[11-13] In most of these studies, the emphasis has been on obtaining detailed surface and flowfield mean properties, although more recently, hot-wire measurements have been made in a two-dimensional (2-D) high Reynolds number reattaching shear layer.[14] One of the objectives of this series of studies is to determine the geometric and flow parameters which control the scales and characteristics of a range of 2-D and 3-D interactions. With these parameters and the flowfield structures known, the hypothesis that such apparently different interactions are members of a single family with certain common properties, may be thoroughly evaluated.

Turbulent interactions such as these are inherently unsteady, although a quantitative knowledge of the degree and physical extent of the unsteadiness is lacking. Their unsteadiness can be seen simply by examining a set of microsecond spark schlieren or shadow photographs taken at random intervals. For a 2-D compression corner, with a shock strength sufficient to induce a separated flow, the unsteadiness appears to be characterized by a slight rippling motion of the wave structure. In contrast, the flowfield ahead of a semi-infinite blunt fin, in the same flow, is extremely steady. Photographs taken using a high speed camera with a framing rate of about 35 kHz[15] have shown that the flowfield is dominated by a randomly-varying shock wave structure, whose motion, involving large amplitude excursions, also appears to be random. Different diameter fins in different incoming

turbulent boundary layers all exhibited this same qualitative behavior. Such a high degree of unsteadiness poses problems for further experiments and clearly has serious implications for computational studies.

Experimentally, few studies have been made of the unsteady characteristics of shock wave turbulent boundary layer interactions. In the main, these experiments have concentrated on the measurement of surface pressure fluctuations in interactions induced by steps and 45° compression corners on axisymmetric bodies[16,17] and by oblique shock waves impinging on a 2-D boundary layer.[18] One of the most extensive studies was that of Robertson[19,20] who tested several circular cylinders of various heights and diameters over the range $0.6 \leq M_\infty \leq 1.6$. None of the cylinders was high enough to be considered semi-infinite and no measurements were made off the centerline, leaving the outboard characteristics unknown. However, these studies have been instrumental in determining r.m.s. pressure distributions and spectral characteristics of attached and separated flows in interactions over a range of incoming flow conditions. The current experiments are concerned with measuring the surface pressure fluctuations in similar blunt fin-induced interactions. Different diameter fins have been tested in different incoming high Reynolds number turbulent boundary layers. Measurements have been made on the centerline and up to four diameters outboard of it. In all cases, the fins used here were high enough to be considered semi-infinite. The criterion necessary for this condition is described in Reference 10.

The aim of this initial set of experiments was to answer some of the basic questions concerning the unsteadiness of blunt fin interactions. Two main areas are addressed by this report. First, the lateral and streamwise extent of the unsteady region and the characteristics within it are

discussed. Second, the dependence of these characteristics on the fin leading edge diameter and incoming turbulent boundary layer are presented.

2. EXPERIMENTAL PROGRAM

Wind Tunnel

All of the tests were carried out in Princeton University's high Reynolds number supersonic, blowdown tunnel. This tunnel has a cross-section 20 cm x 20 cm (8" x 8"), a nominal freestream Mach number of 2.95, and a stagnation pressure range 4×10^5 - 3.4×10^6 Nm^{-2} (60-500 psia).

The tests described here were carried out at a stagnation pressure of 6.8×10^5 Nm^{-2} (100 psia) with a freestream unit Reynolds number of about 6.3×10^7 m^{-1}. In all cases, the tests were made under approximately adiabatic wall conditions.

Model Configurations

The basic model geometry and coordinate system is shown in Figure 1. Two different model configurations were used. The first used the tunnel floor boundary layer which is a 2-D, fully turbulent, equilibrium layer with a nominal thickness of 1.6 cm at the test station. In the second configuration, fins were mounted on a sharp-leading-edged flat plate which spanned the tunnel horizontally. The boundary layer on this plate has been surveyed laterally and streamwise and is 2-D, turbulent and in equilibrium. Tests were made at three positions on the plate. At these locations, the nominal undisturbed boundary layer thicknesses were 0.3 cm, 0.42 cm and 0.52 cm. Further information on these boundary layers is given below. All tests were made with the fin at zero angle of attack.

In both configurations, the floor-mounted pressure transducer was fixed and the sting-mounted fin was moved relative to it. This necessarily meant some small variation in the incoming boundary layer thickness. From previous studies, such variations were known to have a very small effect on the mean properties of the interaction, which are controlled primarily by D.

Any influence on the fluctuation levels could not be easily ascertained *a priori*, although early tests on the flat plate showed that changes in δ of less than about 25% had only a small influence. These are discussed later in the report.

Incoming Turbulent Boundary Layers

The compressible wall-wake law[22] was used as a criterion for judging the condition of the incoming boundary layers. Settles,[2] who used the same tunnel floor and flat plate for studies of compression corner interactions, has shown that the mean velocity profiles fit the wall-wake law well. The skin friction agrees with the van Driest prediction and Λ, the wake strength parameter, falls within the accepted range for equilibrium turbulent boundary layers. On the flat plate model, no boundary layer trips were used; the freestream unit Reynolds number was sufficiently high that transition occurred naturally near the plate leading edge.

Fluctuating Wall Pressure Measurements

The fluctuating pressures were measured using a flush mounted Kulite differential transducer (Model XCQ-062-25D) referenced to vacuum. It is rated for a differential pressure of up to 0.17 MNm^{-2} (25 psi). The sensing element is 0.071 cm (0.028") diameter silicon diaphragm in which a fully active Wheatstone bridge has been bonded atomically. This type of construction has excellent hysteresis and thermal characteristics. The natural frequency is specified by the manufacturer at about 500 kHz, indicating a flat frequency resonse up to about 80 kHz. Measurements by the manufacturer in the lower frequency range of 0-20 kHz confirm the flat response.

The transducer was calibrated statically. Checks made before and after wind tunnel runs showed that the calibration was consistently linear and repeatable. Tests in a shock tube, carried out by Raman,[23] have shown

that transducers employing this type of construction have dynamic calibrations only a few per cent lower than those obtained statically. The transducer signal was amplified, filtered and sampled digitally using a Preston Scientific GMAD-1 A/D converter controlled by an HP1000 mini-computer. Irrespective of sampling rate, data were taken in multiple blocks of 6144 points which were dumped from the computer core to magnetic tape for later analysis.

3. DISCUSSION OF RESULTS

Undisturbed Turbulent Boundary Layer

Many experimental studies have been made of the fluctuating wall pressure characteristics under attached, zero-pressure-gradient turbulent boundary layers. Subsonic, supersonic and hypersonic flows have been studied, with the most detailed information being available at low speed. The broadband r.m.s. pressure levels from such studies are generally presented in nondimensional form ($\langle P_w \rangle / q_\infty$ or $\langle P_w \rangle / \tau_w$) as a function of free-stream Mach number M_∞. Both approaches result in significant scatter, particularly if $\langle P_w \rangle$ is scaled by the local wall shear stress, although this may merely reflect the additional difficulty of accurately measuring or calculating this quantity. Further, such a simple correlation technique does not account for the experimental observations of Raman[23] (also observed in the current study) that at a fixed M_∞, $\langle P_w \rangle / q_\infty$ is a function of q_∞.

Aside from the question of the appropriate correlation parameters, there are many problems associated with such measurements making it difficult to determine a realistic error bar in any particular case. The question of transducer flushness is a critical one. Hanly,[24] made a systematic investigation of this problem at M_∞ = 1.68, 2.0 and 2.5 in the NASA Ames 9' x 7' tunnel. His measurements showed that a slightly protruding transducer caused large effects on the overall r.m.s. pressure level and spectral content whereas a small recess had relatively little effect. At M_∞ = 1.68, a protrusion of 0.4 mm (corresponding to .004δ) increased the overal r.m.s. level 100%. The effect decreased with Mach number: for the same protrusion the error at M_∞ = 2.5 was about 40%. Hanly did not comment on the effects on the mean pressure. In the current study, it was observed that the mean pressure decreased for a small protrusion and increased for a

small recess. For a 0.25 mm protrusion (0.016δ) the decrease was about 10% of the flush value. With an equivalent recess the increase was also about 10%. These and Hanly's results show clearly how critical it is that the transducer be installed flush with the surface, or at worst, slightly recessed.

Further, the higher frequency fluctuations are generally attenuated since pressure transducers necessarily have a finite size. The extent of the error caused by the loss of resolution of the small scale fluctuations is presently unclear. Emmerling's[25] low speed study showed that, when $\langle P_w \rangle / q_\infty$ is plotted versus transducer diameter d scaled by the wall variables (*i.e.* du_τ/ν_w), a large increase (about 100%) in fluctuation intensity occurred for $du_\tau/\nu < \sim 100$. A later study by Bull and Thomas[26] supported the basic conclusion that the transducers used in many studies were too large to detect a significant part of the high frequency fluctuations, but showed that the increase in $\langle P_w \rangle$ at small du_τ/ν_w was not nearly as large as that measured by Emmerling. The increase in intensity for $du_\tau/\nu_w < \sim 100$ was determined by them to be between 20 to 40%. Under the present conditions, and those of other high speed studies, the lowest value of du_τ/ν_w obtainable with the smallest available transducer is of order several hundred, so the possibility of an increase in intensity for small du_τ/ν_w cannot be determined.

Results in the form $\langle P_w \rangle / q_\infty$ versus M_∞ for the current study and several others[17,18,27,28,29] are shown in Figure 2. All the results shown are for adiabatic wall boundary layers. [In the case of cold walls, Raman's[23] measurements show substantially higher intensities than would be expected from the adiabatic correlation.] Only results for which $M_\infty > 1$ are shown in the figure. The subsonic data can be correlated, within a reasonable amount of scatter, by the simple expression $\langle P_w \rangle / q_\infty = 0.006$. Lowson[30] and

Laganelli, *et al.*,[31] have both developed semi-empirical expressions for predicting the pressure fluctuations in zero-pressure-gradient supersonic and hypersonic turbulent boundary layers. Both expressions are of the form:

$$\frac{\langle p_w \rangle}{q_\infty} = \frac{0.006}{(1 + a\, M_\infty^2)^b}$$

where a = 0.14, b = 1 in Lowson's formulation and a = 0.13, b = 0.64 in Laganelli's formulation. Both predictions, shown as solid curves on the figure, tend to be consistently higher than most of the data.

Power spectra for attached turbulent boundary layers have been found to scale on an appropriate Strouhal Number. The frequency is made non-dimensional by multiplying by a typical length and dividing by a typical velocity. Usually, freestream velocity U_∞ is used for the latter, whereas δ, δ^* and θ have been used as length scales. The power axis is generally non-dimensionalized using U_∞ and one of the above length scales in combination with q_∞^2 or τ_w^2. Chyu and Hanly[32] noted that using τ_w correlated spectral curves better at the higher frequencies, supporting the argument that the turbulence of high frequency eddies is dominated by viscous forces that exist near the wall.

In general, attempts to normalize spectra over a broad range of flow conditions have resulted in a wide data spread. The difficulties are exemplified by the study of Lewis, *et al.*,[33] in which twelve different transducers were used on the wall of the NASA-Ames 9' x 7' tunnel at Mach numbers of 1.6, 2.0 and 2.5. The results shown in Figure 3 illustrate the data spread. Bies,[34] attempted to correlate data obtained by many different investigators using different transducers over a wide range of

Mach numbers ($0.03 \leq M_\infty \leq 3.96$) and Reynolds numbers. The data spread obtained by Bies and the line of greatest data cluster are also shown on Figure 3. Data from the present tests on the tunnel floor (δ = 1.6cm, $Re_\delta = 10^6$) are shown by the heavy solid line.

Fin Centerline Characteristics

Figure 4 shows the normalized r.m.s. ($\langle P_w \rangle / \langle P_\infty \rangle$) and mean ($P_w/P_\infty$) pressure distributions on centerline ahead of a 1.27 cm diameter fin. The incoming turbulent boundary layer is 1.6 cm thick. Two sets of mean pressures are shown. One is the calculated mean from the fluctuating pressure signal of the Kulite transducer. The other was measured in a previous study[12] using the conventional technique of surface tappings and a scanivalve. The two techniques agree well.

The X axis is scaled by D, since the earlier studies[11,12] have shown that it is the appropriate parameter for correlating centerline mean pressure distributions. Large changes in incoming boundary layer thickness (for a fixed diameter fin) have been shown to result only in second order changes in the interaction scale and characteristics, not only on the centerline, but up to several diameters outboard.

As an aid to the general description of the centerline characteristics, several pressure-time histories and corresponding probability density distributions are shown in Figures 5 and 6. The pressure-time plots, with the pressure normalized by the upstream undisturbed mean static level, each consist of 6144 points (1 data file). For comparative purposes, the scale of the pressure axis is kept constant. Six files were used to calculate each probability density distribution. The solid line on the probability density plots is the normalized Gaussian distribution given by

$$P(z) = (\sqrt{2\pi})^{-1} e^{-z^2/2}$$

where $$z = \frac{P_w(t)-P_w}{\sigma P_w}$$

where σP_w is the standard deviation of the signal.

Upstream of the first peak in the r.m.s. pressure distribution (labelled P_{R_1} in Fig. 4) the pressure time histories at X/D = -2.75 and -2.5 (Figs. 5b and 5c, respectively) show the motion of a compression wave system. At X/D = -2.75, the trace shows mainly the undisturbed turbulent boundary layer with pressure "spikes" or "pulses" superimposed on it. Four schlieren photographs of the flowfield ahead of the fin root are shown in Figure 7. These were taken at random intervals using a microsecond spark light source. Significant variations in the wave pattern occur from frame to frame.

At X/D = -2.75 the one-sidedness caused by the "spikes" exists for only a small fraction of the total time. It raises the mean pressure only a few percent above the undisturbed level, but substantially increases the r.m.s. level of the fluctuations. The small increase in the mean results in most of the signal (consisting of the undisturbed boundary layer) being close to, but below, the mean value. This type of pressure distribution radically alters the probability density distribution (Fig. 6b).

At X/D = -2.5, close to P_{R_1}, the one-sidedness occurs more frequently and for longer time spans, increasing both the mean and r.m.s. pressure levels still further. The pressure increments $\Delta P[=P(t)/P_\infty)-1]$ caused by the one-sidedness is around 0.7-1.2, which, if caused by a single shock wave, would correspond to wave angles in the range 25°-29° at this M_∞. This is typical of the angles measured from the schlieren photographs.

Even at this location, a significant fraction of the total time is still spent at effectively undisturbed conditions. Since the mean value is about 20% higher than the undisturbed level, this results in the highest probability occurring at around $-1\sigma p_w$ from the mean. The slight bulge in the distribution at around $+ 1.25\sigma p_w$ occurs because the higher mean and fluctuating levels corresponding to conditions downstream of the wave system are occurring more frequently. Further downstream, at X/D = -2.4D and-2.3D, the sharp peak A of Figure 6b decreases rapidly and the bulge B (same figure) develops into a well-defined peak.

The dynamic character of the flowfield in this region could not have been inferred from a mean pressure distribution alone. The time varying surface pressure plots show a flowfield rapidly and randomly alternating between that associated with an undisturbed turbulent boundary layer and that corresponding to the downstream region of a complex compression wave system. This wave structure undergoes random excursions over significant streamwise distances and generates high-intensity pressure fluctuations. Ahead of the r.m.s. peak, P_{R1}, the mean pressure steadily increases, but this is the result of averaging two rather distinct signals. In this region, an increase in the mean simply implies that the signal spends less time in the undisturbed mode, whereas in a purely Gaussian process it would correspond to an upward shift in the entire signal.

To obtain an accurate idea of the dynamic behavior, a probability distribution (or pressure-time history) is needed in addition to the mean distribution. For example, upstream influence L_u, determined from the mean pressure distribution of Figure 4a, is at approximately X/D = -2.75. From the dynamic point of view, Figures 5b and 6b show that the pressure

level at this position is above the undisturbed value only about 10% of the total time. At this point, which, from the mean point of view, is the interaction start, the flowfield is undisturbed around 90% of the time. At X/D = -2.5, P_w/P_∞ is about 1.2, but even here, the flowfield is essentially undisturbed for a significant fraction of the total time. Even at X/D = -2.25, where $P_w/P_\infty \sim 1.5$, there are instances when the wave system is further downstream leaving the local flowfield undisturbed (*i.e.* point A of Figure 5d). This behavior shows up on the probability distribution as a small peak at around $-2.5\sigma p_w$ from the mean.

Downstream of P_{R_1}, the one-sided nature of the pressure trace disappears, and at X/D = -2.0, where a minimum in $\langle P_w \rangle / \langle P_\infty \rangle$ occurs, the probability distribution becomes Gaussian. As the r.m.s. level steadily increases from here to around X/D = -1.25, the probability remains Gaussian. At X/D = -1.0 (Fig. 6f), the probability again acquires the characteristic associated with a one-sided signal. This can be seen from the pressure time history of Figure 5f. The physical cause of this is not clear. The branch of the bow shock beneath the triple point is unsteady, but from schlieren photographs (Fig. 7) does not appear to move far enough upstream to be the cause of this result. Closer to the leading edge, at $X/D \sim -0.25$, the same type of probability distribution reappears and it is possible that in this case this shock is the cause.

The r.m.s. and mean pressure distributions shown in Figure 4 are qualitatively similar to those measured by Robertson[19,20] ahead of a circular cylinder at $M_\infty = 1.6$. The cylinder was not quite high enough to be considered semi-infinite, but was close to this condition. R.m.s. pressure peak P_{R_1} (see Fig. 4) was not resolved in these measurements, but peaks 2 and 3 were, and were approximately equal with $\langle P_w \rangle / \langle P_\infty \rangle$ being

about 16. Further, r.m.s. peaks 2 and 3 and the trough between peaks 1 and 2 occurred at about the same locations in the mean pressure distribution as observed in the current tests.

Based on these distributions, in conjunction with surface oil streak patterns, Robertson proposed a model for the flowfield ahead of the cylinder: downstream of the unsteady shock structure, the boundary layer separates, with the formation of a system of horseshoe vortices below the separated shear layer. Winkelmann[35] has proposed a similar model. At low speeds ($\sim$ 2 m/s) with a laminar boundary layer this structure does exist, as shown by the smoke visualization studies of Norman.[36] It's existence at transonic or supersonic speeds is an open question since, as far as is known, no flowfield or flow visualization results are available.

In Robertson's model, P_{R_2} lies between the two major vortices. He proposed that the shear interaction due to opposite velocity vectors generates the intense pressure fluctuations. Upstream of this peak, the mean static pressure in his distribution did not vary significantly, and this was interpreted as being due to an elongated vortex underneath the separated shear layer. The separation point occurred immediately downstream of the unsteady shock structure and was indicated by an accumulation of oil in the surface flow patterns. Since Robertson only made measurements on the centerline it is not possible to see if the correlation between the r.m.s. and mean pressures and the surface pattern persisted in some rational way further outboard. In the current study, measurements were made on and off centerline and surface flow patterns of this region were obtained using a kerosine-lampblack method.[3] These are discussed in a later section.

Compared to 2D interactions, such as those induced by steps, there are both similarities and differences between the r.m.s. pressure distributions.

Chyu and Hanly's experiments, using a 2D step ($h/\delta = 2$) in a Mach 2.5 flow, show that close to the interaction start there is a peak in the r.m.s. distribution corresponding to P_{R1}. The peak value was not resolved but a linear extrapolation of the data suggests a value of $\langle P_w \rangle / \langle P_\infty \rangle$ of about 35 to 40. This is higher than that in Figure 4, but the fin results (as discussed later) depend on the ratio D/δ, and, under the appropriate conditions, P_{R1} can be that high. In the step case, the value of $\langle P_w \rangle / \langle P_\infty \rangle$ is constant throughout the separated flow regime and almost independent of Mach number. No measurements were made close to the step face so the distribution in this region is unknown. Similar results were obtained by them with a 45° 2D compression corner. In this case, very intense fluctuation levels ($\langle P_w \rangle / \langle P_\infty \rangle$ of order 50) were measured in the reattachment region.

These 2D geometries and the blunt fin all have a highly unsteady shock structure at the upstream boundary of the interaction. The step and compression corner, which have similar separated flows, have similar r.m.s. characteristics in the separated flow regions. These differ from those of the blunt fin, indicating that although the centerline region may have a quasi-two-dimensional nature, the structure of the separation flow region is certainly different.

Lateral and Streamwise Extent of Unsteady Region

Measurements of fluctuating surface pressures were made along rows parallel to the centerline at values of Y/D up to 4. Using these, contours of constant $\langle P_w \rangle / \langle P_\infty \rangle$ were constructed and are shown in Figure 8. Upstream of the contour given by $\langle P_w \rangle / \langle P_\infty \rangle = 1$, the boundary layer is undisturbed. For reference purposes, the undisturbed bow shock wave is also shown.

For comparison purposes, mean wall pressure contours, measured in an earlier study, are shown in Figure 9. The characteristic double peaked

pressure dsitribution seen on centerline (Fig. 4) extends outboard at least 4D. The two pressure peaks, one upstream of the bow shock wave, and one downstream of it, both decay outboard of the centerline. P_{M_1}, the upstream peak, decreases slowly, with earlier studies showing that at Y/D = 100, $\Delta P \sim 0.1$. The downstream peak P_{M_2} decreases rapidly from $\Delta P \sim 5$ on centerline to about 1 at Y/D = 1.5. At Y/D = 4 it is barely discernible. The trough between the two peaks decreases slowly with increasing Y/D and shifts from ahead of the bow shock on centerline to behind it around Y/D $\sim$ 2 to 3.

In an analogous way, the outboard r.m.s. pressure distributions exhibit similar characteristics to those seen on centerline. With increasing Y/D, the intensity of the fluctuations decreases. At Y/D of 4 it is still significantly above the level of the incoming boundary layer. P_{R_1} decreases from a value of $\langle P_w \rangle / \langle P_\infty \rangle \sim 20$ on centerline to about 12 at Y/D = 4, indicating that the unsteady wave structure ahead of the main shock wave extends a significant distance outboard. P_{R_2} decreases more rapidly from a well-defined peak on centerline ($\langle P_w \rangle / \langle P_\infty \rangle \sim 20$) to a small "hump" ($\langle P_w \rangle / \langle P_\infty \rangle \sim 5$) in the distribution at Y/D = 4. The resolution of the measurements was insufficient to characterize accurately the third peak, but the decay is extremely rapid.

As a general observation, the fluctuations are more intense ahead of the bow shock wave than behind it. Upstream, the contours are closely spaced and large gradients occur, particularly in the region close to, and around, the leading edge. Downstream of the bow shock wave, the fluctuation intensity progressively decreases. Within 6D, the level has relaxed to about twice that of the incoming boundary layer. In contrast, the mean

distribution is more "symmetric" about the bow shock wave, with a peak occurring both upstream and downstream of it.

Correlation of Mean and R.M.S. Pressure Distributions with the Surface Flow Pattern

The kerosine-lampblack method was used for obtaining surface flow patterns. An example is shown in Figure 10. This technique has effectively zero frequency response. The fine detail available in the original trace does not reproduce well, but certain features may be seen. To aid the following discussion, characteristics such as the peaks and troughs of the r.m.s. and mean pressure distributions and features from this surface flow pattern are shown in Figure 11.

The turning of the originally-parallel surface streaks defines the extent of mean upstream influence, and correlates with the initial rise in the mean pressure distribution. Downstream of this turning, the unsteady wave structure effectively "sweeps" the surface clean, leaving it uniformly gray. The downstream boundary of this region is a well-defined line, generally referred to as the "primary separation" line. The r.m.s. pressure peak P_{R1} occurs in this region and lies roughly mid-way between the line defining the mean upstream influence and the "primary separation" line.

The "primary separation" line does not result from the accumulation of lampblack, but is a dividing line and appears sharply defined on account of the shading contrast between the two regions that it separates. It lies ahead of the contour defining the mean peak pressure P_{M1} but moves progressively closer as Y/D increases. In terms of mean pressure levels, it corresponds to a P_w/P_∞ of about 1.7 on centerline to about 1.6 at Y/D = 4. Whether or not this line represents separation of the incoming boundary layer can only be properly answered through surveys or flowfield visualization.

Certain observations do tend to support a separated flow interpretation. In the vicinity of the centerline, the bow shock and this line are approximately normal to the incoming flow, and locally, the disturbed flow regime may have a quasi-two-dimensional character. Earlier evidence indicates major differences in the separated regime, but in the approach to the "separation line", two-dimensional ideas may apply. Two-dimensional compression ramp studies[3] using the same incoming boundary layer, show that the pressure ratio at separation is close to 1.7 to 1.8. This corresponds closely to the values given above, particularly near the centerline. Further, observations of the developing kerosine-lampblack patterns near the leading edge show a reverse flow close to the surface. Initially, the streaks move upstream with only a small transverse component. Within a short distance, a large transverse component develops and they are swept outboard and downstream.

The second r.m.s. pressure peak P_{R_2} lies ahead of and close to the trough in the mean pressure distribution. A close examination of the streak pattern shows that this trough occurs at the location of the maximum streak angle, as shown in Figure 12. The surface streak angle, β, is measured relative to the undisturbed flow direction. Checks made at other values of Y/D consistently show the same behavior. The maximum β occurs close to the bow shock wave and decreases rapidly downstream. Typically, within two to four diameters further downstream, β is close to zero. The r.m.s. pressure peak, P_{R_2}, which occurs just upstream of this maximum oil streak angle, may result from the intense shearing associated with extremely large yaw angle gradients near the wall.

Downstream of P_{R_2}, the r.m.s. pressure level progressively decreases, as does β, although the mean pressure rises to a second peak P_{M_2} and then

decays gradually. It is difficult to discern on the streak pattern, but the locus of P_{M_2} corresponds to a line about which the streaks diverge. This divergence line is often interpreted as being a "reattachment line." However, unlike the 2-D case, where the r.m.s. pressure level rises rapidly through the reattachment process, here it progressively decreases throughout this region.

These results show that in moving progressively outboard, certain features of the r.m.s. and mean pressures correlate and also correspond to certain characteristics of the surface streak pattern. The upstream region is bounded by a unsteady compression/shock structure resulting in high intensity pressure fluctuations. Downstream of this there is a strong indication that flow separation occurs, at least in the neighborhood of the centerline. The physical nature of the separation and details of the flowfield are difficult to infer with any measure of confidence from the surface properties alone.

Effects of Fin Leading Edge Diameter and Incoming Boundary Layer Thickness

Centerline mean pressure distributions for D = 1.27 cm and 2.54 cm are shown in Figure 13a. These are the averaged Kulite signals and agree well with those from surface taps. They exhibit the characteristic trends associated with increasing D/δ, namely a decrease in mean upstream influence and an increase in the pressure level of the upstream peak (P_{M_1}).

The corresponding r.m.s. pressure distributions, normalized by $\langle P_\infty \rangle$, are shown in Figure 13b. They both have the same characteristic features which correlate well with the X axis normalized by D. In general, at a given station, the larger fin generates higher intensity fluctuations. Quantitatively, the ratio of intensities at the peaks is difficult to define,

since their precise locations are experimentally difficult to resolve.

Both of these fins were tested on the flat plate with a 0.3 cm thick incoming boundary layer. Mean and r.m.s. pressure distributions for the 1.27 cm diameter fin are shown in Figures 14a and 14b. The mean distributions show the changes which would be predicted when D/δ is increased by a factor of 4. The r.m.s. distributions have similar features and, although in terms of X/D the peaks and troughs do not correspond, their relative positions on the mean distribution are essentially the same. Overall, the thinner boundary layer case has the higher intensity fluctuations.

These results suggest that the effects of changes in D and δ can be combined by considering the single parameter D/δ. In addition, a simple dimensional analysis shows that these are the two characteristic lengths in the interaction. Upstream influence and centerline and fin leading edge pressure distributions are all dependent primarily on D. For a fixed δ, doubling D, as in Figure 13, approximately doubles the physical streamwise and vertical extent of the interaction. This means that a larger fraction of the wave structure ahead of the fin root is effectively outside of the boundary layer. The same result occurs if D is fixed and δ progressively decreased. The pressure-time histories show that when the wave system is predominantly immersed in the boundary layer (*i.e.* low D/δ), the amplitude of the "spikes" is reduced. Further, the structure tends to be more dispersed, consisting of series of waves, rather than a single, stronger shock. This results in a higher r.m.s. pressure level at the first peak P_{R_1} as the ratio D/δ increases.

4. CONCLUDING REMARKS

An experimental study has been made of the unsteady surface pressure characteristics of blunt fin-induced shock wave turbulent boundary layer interaction. Different diameter fins have been used in different incoming turbulent boundary layers. All tests were made at a freestream Mach number of 2.95, a unit Reynolds number of 6.3×10^7 m^{-1} and under approximately adiabatic wall conditions. These measurements have shown that:

a) The flowfield in the vicinity of the fin leading edge is characterized by a highly unsteady shock wave structure. This structure varies continually with the waves forming it undergoing random streamwise excursions over a distance of about 1D.

b) On centerline the r.m.s. pressure distribution has three distinct peaks. These peaks, and the overall r.m.s. pressure level, all decrease with distance outboard.

c) The upstream r.m.s. pressure peak is caused by the unsteady wave structure. The r.m.s. levels at this peak are up to forty times that of the incoming boundary. This is comparable to that observed in 2-D step induced interactions. The peak occurs close to the mean upstream boundary of the interaction. At 4D outboard it has only decreased by about 50%, indicating that this unsteady structure extends a significant distance off centerline.

d) The second peak, which correlates approximately with the maximum surface streak angle seen on kerosine-lampblack patterns, decreases rapidly outboard and is barely discernible at Y/D of 4.

e) The third peak, which occurs close to the fin root, has an r.m.s. level up to two orders of magnitude higher than that of the incoming boundary

layer. This peak is swept around the fin leading edge and decreases extremely rapidly. At 2D outboard it is not detectable.

f) The region upstream of the bow shock wave is characterized by intense fluctuation levels and steep gradients in r.m.s. pressures. In sharp contrast, the r.m.s. level downstream of the bow shock steadily decreases. Within six to eight diameters in the streamwise direction it is close to that of the incoming boundary layer.

g) The overall fluctuation levels throughout the interaction depend on both the fin leading edge diameter and the incoming boundary layer thickness. The intensity of the fluctuations increase with increasing D/δ. Physically, when D/δ is small, the wave structure is predominantly immersed in the incoming boundary layer. This tends to smear out the wave system and results in lower fluctuation levels.

REFERENCES

1. Settles, G. S., Perkins, J. J. and Bogdonoff, S. M., "Investigation of Three-Dimensional Shock/Boundary-Layer Interactions at Swept Compression Corners," *AIAA Journal*, Vol. 18, July 1980, pp. 779-785.

2. Settles, G. S., Perkins, J. J. and Bogdonoff, S. M., "Upstream Influence Scaling of 2D and 3D Shock/Turbulent Boundary Layer Interactions at Compression Corners," AIAA Paper No. 81-334, January 1981.

3. Settles, G. S., "An Experimental Study of Compressible Turbulent Boundary Layer Separation at High Reynolds Number," Ph.D. Dissertation, Aerospace and Mechanical Sciences Dept., Princeton University, Princeton, NJ, Sept. 1975.

4. Settles, G. S., Bogdonoff, S. M. and Vas, I. E., "Incipient Separation of a Supersonic Turbulent Boundary Layer at High Reynolds Numbers," *AIAA Journal*, Vol. 14, Jan. 1976, pp. 50-56.

5. Settles, G. S., Vas, I. E. and Bogdonoff, S. M., "Details of a Shock Separated Turbulent Boundary Layer at a Compression Corner," *AIAA Journal*, Vol. 14, No. 12, December 1976.

6. Horstman, C. C., Settles, G. S., Vas, I. E., Bogdonoff, S. M. and Hung, C. M., "Reynolds Number Effects on Shock-Wave Turbulent Boundary Layer Interactions," *AIAA Journal*, Vol. 15, No. 8, Aug. 1977, pp. 1152-1158.

7. Settles, G. S., Fitzpatrick, T. J. and Bogdonoff, S. M., "Detailed Study of Attached and Separated Compresion Corner Flowfields in High Reynolds Number Supersonic Flow," *AIAA Journal*, Vol. 17, June 1979, pp. 579-585.

8. Oskam, B., Bogdonoff, S. M. and Vas, I. E., "Study of Three-Dimensional Flow Fields Generated by the Interaction of a Skewed Shock Wave with a Turbulent Boundary Layer," AFFDL-TR-75-21, Feb. 1975.

9. Oskam, B., Vas, I. E. and Bogdonoff, S. M., "Mach 3 Oblique Shock Wave/Turbulent Boundary Layer Interactions in Three Dimensions," AIAA Paper No. 76-336, July 1976.

10. Dolling, D. S. and Bogdonoff, S. M., "Upstream Influence Scaling of Sharp Fin-Induced Shock Wave Turbulent Boundary Layer Interactions," AIAA Paper No. 81-0336, January 1981.

11. Dolling, D. S., Cosad, C. D. and Bogdonoff, S. M., "Three-Dimensional Shock Wave Turbulent Boundary Layer Interactions - A Parametric Study of Blunt Fin-Induced Flows," AIAA Paper 78-159, January 1978.

12. Dolling, D. S., Cosad, C. D. and Bogdonoff, S. M., "An Examination of Blunt Fin-Induced Shock Wave Turbulent Boundary Layer Interactions," AIAA Paper No. 79-0668, January 1979.

13. Dolling, D. S. and Bogdonoff, S. M., "Scaling of Interactions of Cylinders with Supersonic Turbulent Boundary Layers," *AIAA Journal*, Vol. 19, No. 5, May 1981.

14. Settles, G. S., Baca, B. K., Williams, D. R. and Bogdonoff, S. M., "A Study of Reattachment of a Free Shear Layer in Compressible Turbulent Flow," AIAA Paper 80-1408, July 1980.

15. Degrez, G., "Exploratory Experimental Investigation of the Unsteady Aspects of Blunt Fin-Induced Shock Wave Turbulent Boundary Layer Interactions," M.S.E. Thesis (1516-T), Mechanical and Aerospace Engineering Dept., Princeton University, Princeton, NJ, June 1981.

16. Coe, C. F., Chyu, W. J. and Dods, J. B., "Pressure Fluctuations Underlying Attached and Separated Supersonic Turbulent Boundary Layers and Shock Waves," AIAA Paper No. 73-996, Aero-Acoustics Conference, Seattle, Washington, October 1973.

17. Chyu, W. J. and Hanly, R. D., "Power and Cross Spectra and Space-Time Correlations of Surface Fluctuating Pressures at Mach Numbers Between 1.6 and 2.5," AIAA Paper No. 68-77, January 1968.

18. Speaker, W. V. and Ailman, C. M., "Spectra and Space-Time Correlations of the Fluctuating Pressures at a Wall Beneath a Supersonic Turbulent Boundary Layer Perturbed by Steps and Shock Waves," NASA CR-486, May 1966.

19. Robertson, J. E., "Characteristics of the Static and Fluctuating-Pressure Environments Induced by Three-Dimensional Protuberances at Transonic Mach Numbers," Wyle Laboratories Research Staff Report WR-69-3, June 1969.

20. Robertson, J. E., "Prediction of In-Flight Fluctuating Pressure Environments Including Protuberance Induced Flow," Wyle Laboratories Research Staff Report WR-71-10, March 1971.

21. Dolling, D. S., Cosad, C. D. and Bogdonoff, S. M., "Three-Dimensional Shock Wave Turbulent Boundary Layer Interactions - A Preliminary Analysis of Blunted Fin-Induced Flows," Report 1354, MAE Dept., Princeton University, October 1977.

22. Sun, C. C. and Childs, M. E., "A Modified Wall Wake Velocity Profile for Turbulent Compressible Boundary Layers," *AIAA Journal of Aircraft*, Vol. 10, June 1973, pp. 381-383.

23. Raman, K. R., "A Study of Surface Pressure Fluctuations in Hypersonic Turbulent Boundary Layers," NASA-CR-2386, February 1974.

24. Hanly, R. D., "Effects of Transducer Flushness on Fluctuating Surface Pressure Measurements," AIAA Paper No. 75-534, 2nd Aero-Acoustics Conference, Hampton, Va., March 1975.

25. Emmerling, R., Meier, G. E. A. and Dinkelacker, A., "Investigation of the Instantaneous Structure of the Wall Pressure Under a Turbulent Boundary Layer Flow," A.G.A.R.D. Conf. Proceedings 131 on Noise Mechanism, Paper No. 24.

26. Bull, M. K. and Thomas, A. S. W., "High Frequency Wall-Pressure Fluctuations in Turbulent Boundary Layers," *The Physics of Fluids*, Vol. 19, No. 4, April 1976.

27. Roberts, D. R., "Boundary Layer Pressure Fluctuations at High Reynolds Numbers on a Second Free-Flight Test Vehicle," Aeronautical Research Council, ARC CP No. 1302, 1974.

28. Lewis, T. L., Dods, Jr., J. B., and Hanly, R. D., "Measurements of Surface Pressure Fluctuations on the XB-70 Airplane at Local Mach Numbers up to 2.45," NASA TN D-7226, March 1973.

29. Richards, E. J., Bull, M. K. and Willis, J. L., "Boundary Layer Noise Research in the U.S.A. and Canada - A Critical Review," A.R.C. 21,766, February 1960.

30. Lowson, M. V., "Prediction of Boundary Layer Pressure Fluctuations," AFFDL-TR-67-167, April 1978.

31. Laganelli, A. L., Martellucci, A. and Shaw, L., "Prediction of Surface Pressure Fluctuations in Hypersonic Turbulent Boundary Layers," AIAA Paper No. 76-409, July 1976.

32. Chyu, W. J. and Hanly, D. H., "Power and Cross Spectra and Space Time Correlations of Surface Fluctuating Pressures at Mach Numbers Between 1.6 and 2.5," NASA TN-D-5440, September 1969.

33. Lewis, T. L. and Dods, Jr., J. B., "Wind Tunnel Measurements of Surface-Pressure Fluctuations at Mach Numbers of 1.6, 2.0 and 2.5 Using Twelve Different Transducers," NASA TN-D-7087, October 1972.

34. Bies, D. A., "A Review of Flight and Wind Tunnel Measurements of Boundary Layer Pressure Fluctuations and Induced Structural Response," NASA CR-626, October 1966.

35. Winkelmann, A. E., "Flow Visualization Studies of a Fin Protuberance Partially Immersed in a Turbulent Boundary Layer at Mach 5," NOLTR-70-93, May 1970.

36. Norman, R. S., "On Obstacle Generated Secondary Flows in Laminar Boundary Layers and Transition to Turbulence," Ph.D. Thesis, Illinois Institute of Technology, December 1972.

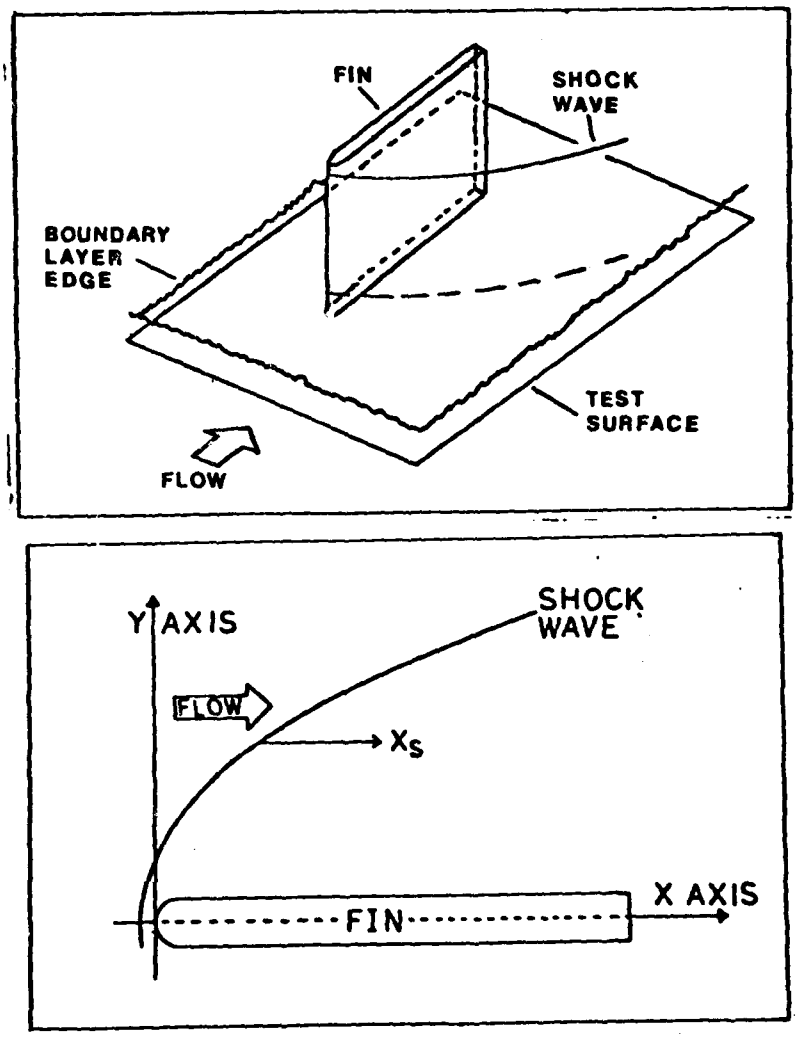

Figure 1. Model Geometry and Coordinate System.

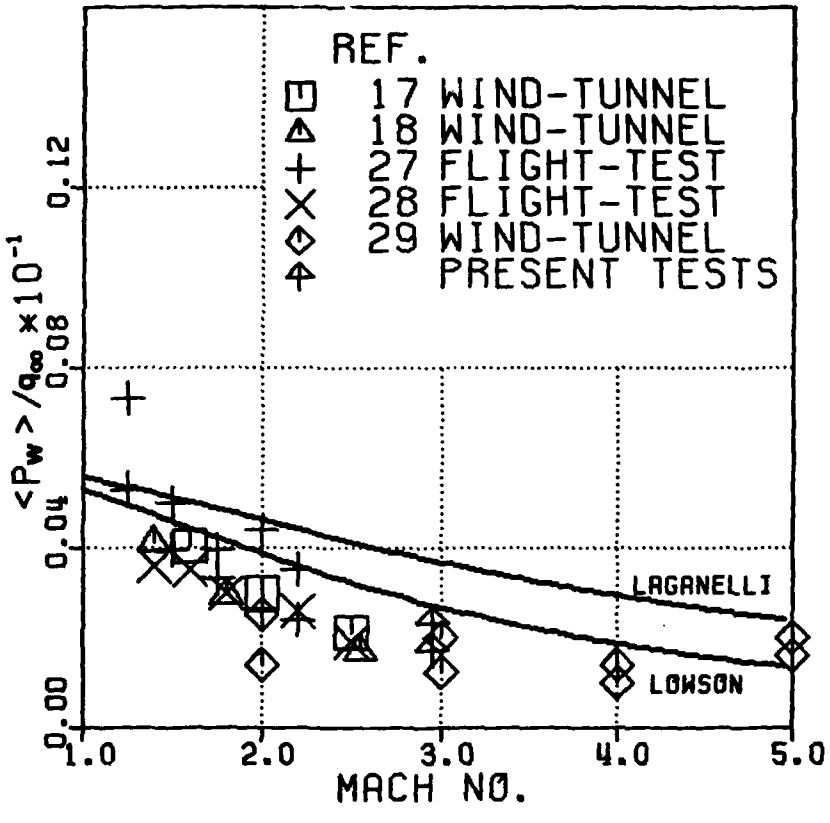

Figure 2. $<P_w>/q_\infty$ for Attached Turbulent Boundary Layers as a Function of Freestream Mach Number.

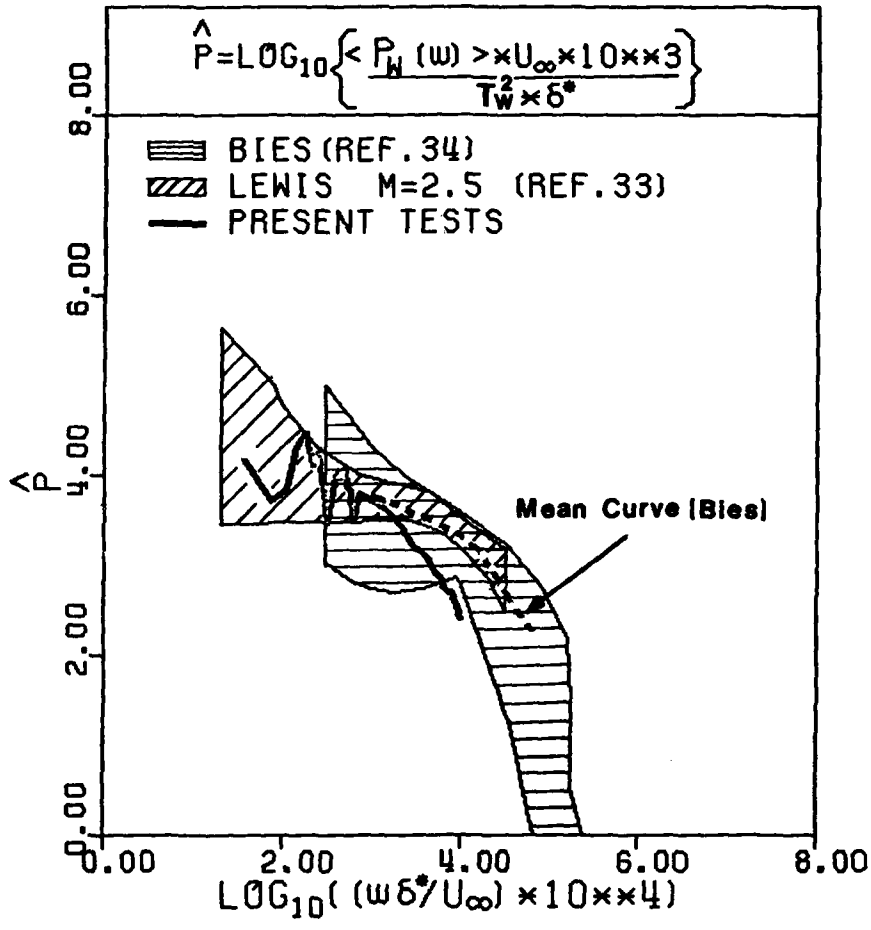

Figure 3. Power Spectra of Undisturbed Turbulent Boundary Layer Pressure Fluctuations.

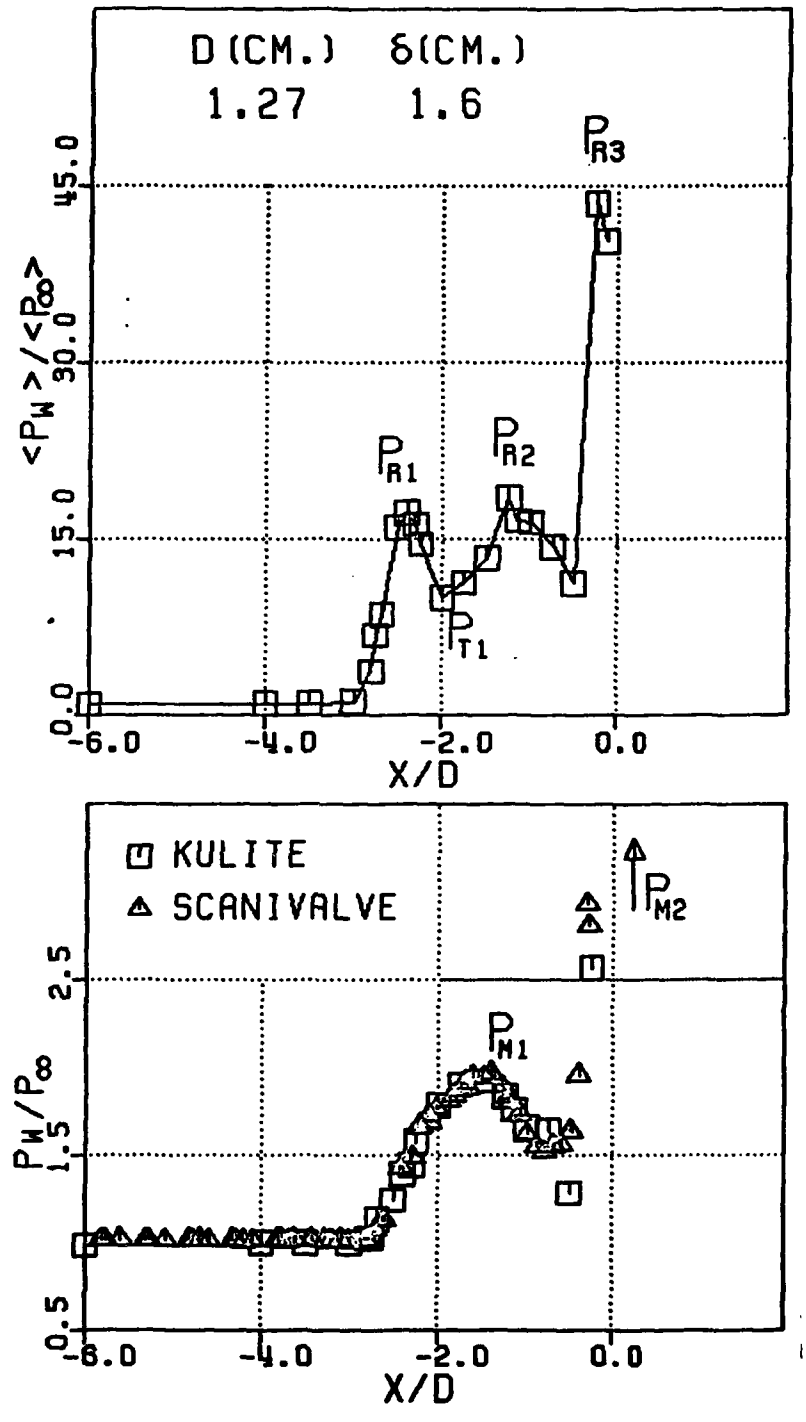

Figure 4. Normalized R.M.S. and Mean Pressure Distributions on Fin Centerline.

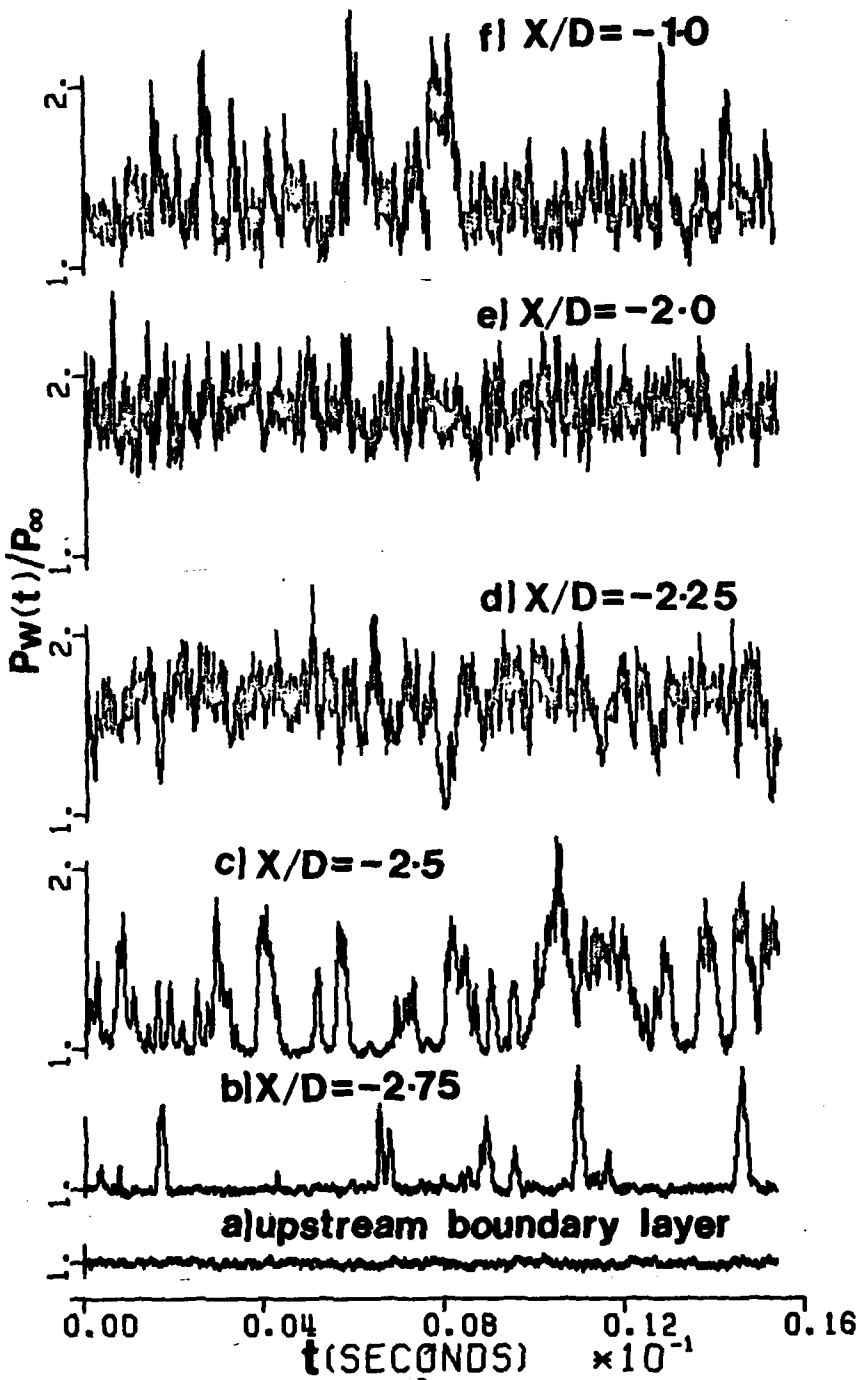

Figure 5. Samples of Pressure-Time Histories on Fin Centerline.

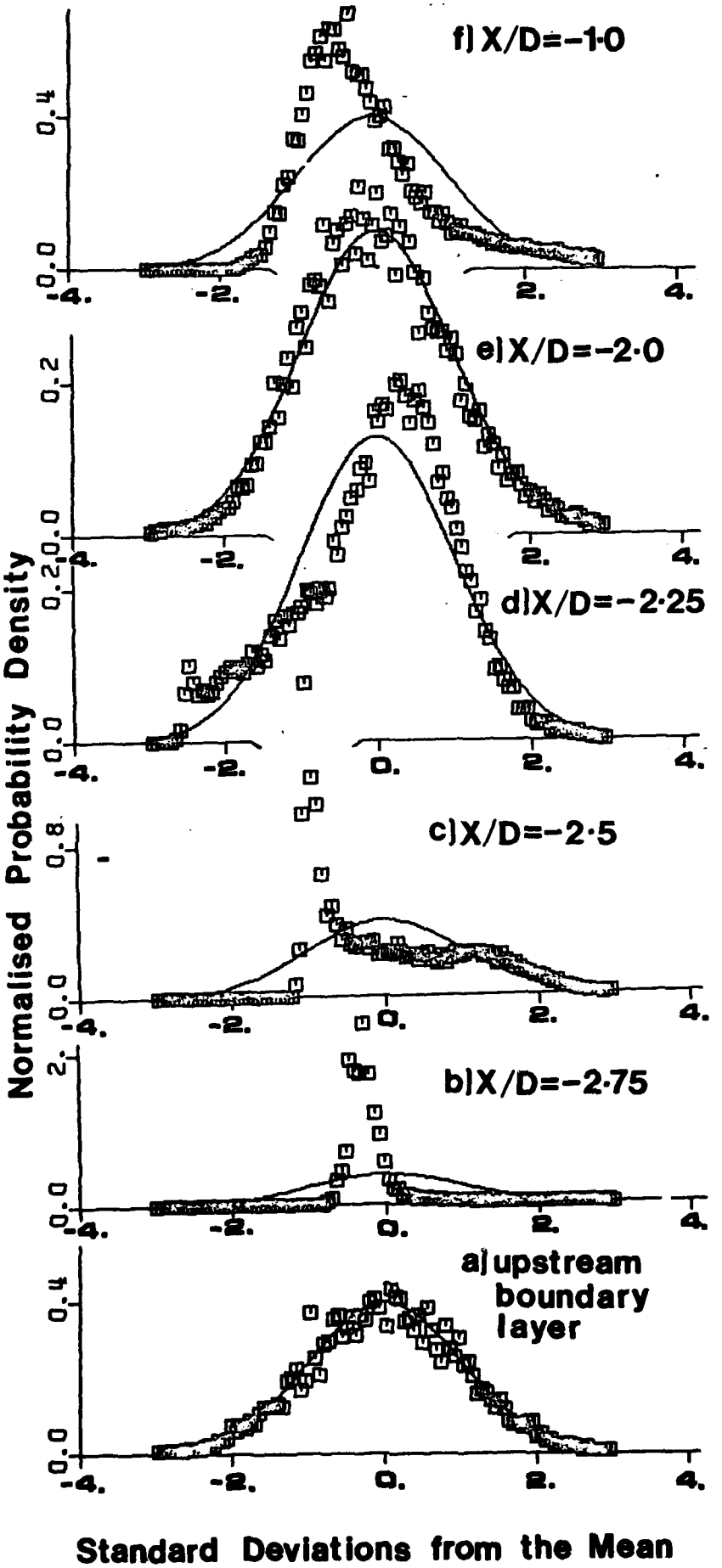

Figure 6.

Probability Density Distributions on Fin Centerline.

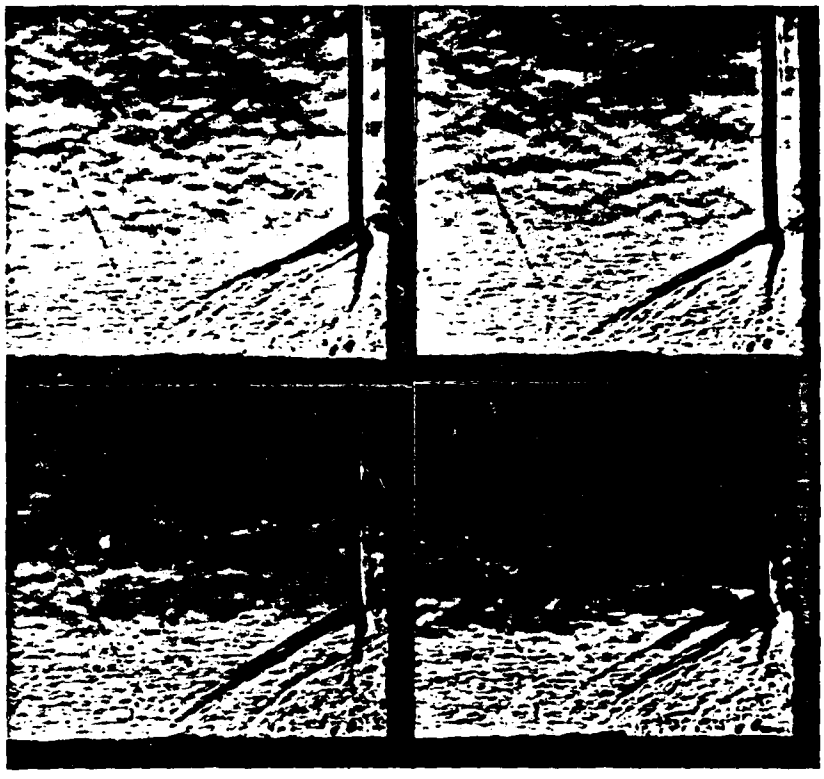

Figure 7. Shock Wave Structures Upstream of the Fin.

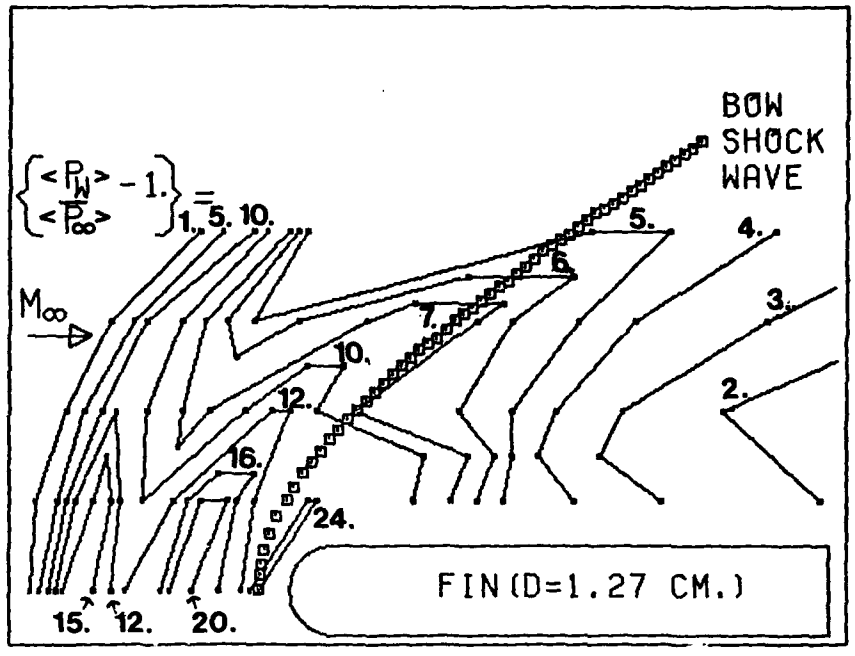

Figure 8. Normalized R.M.S. Pressure Contours.

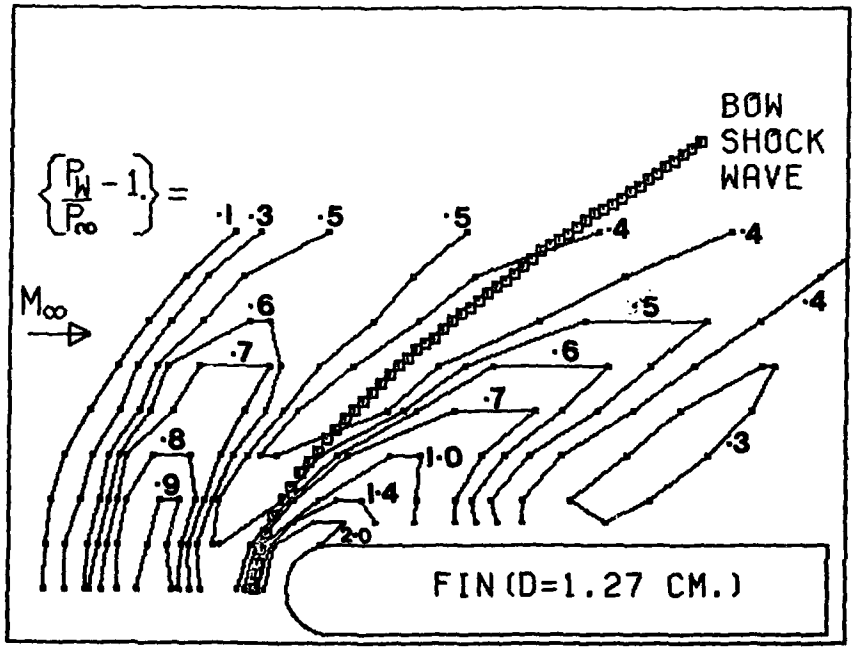

Figure 9. Normalized Mean Pressure Contours.

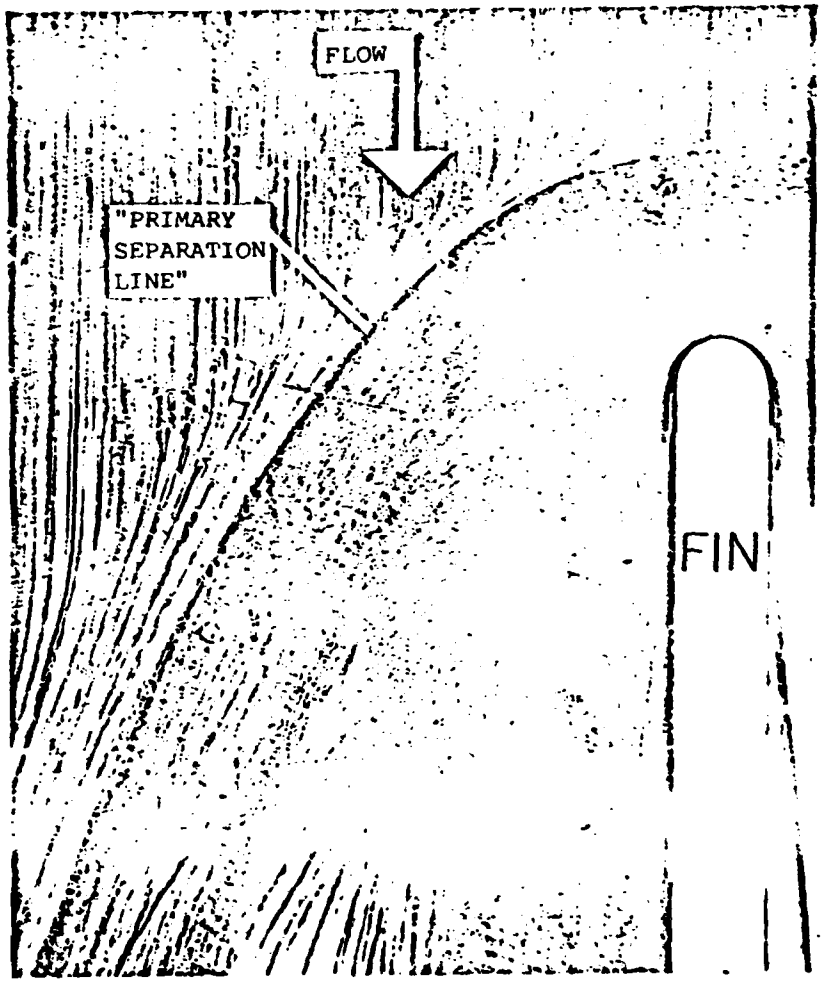

Figure 10. Kerosine-Lampblack Surface Flow Pattern
(D = 1.27cm, δ = 1.6cm)

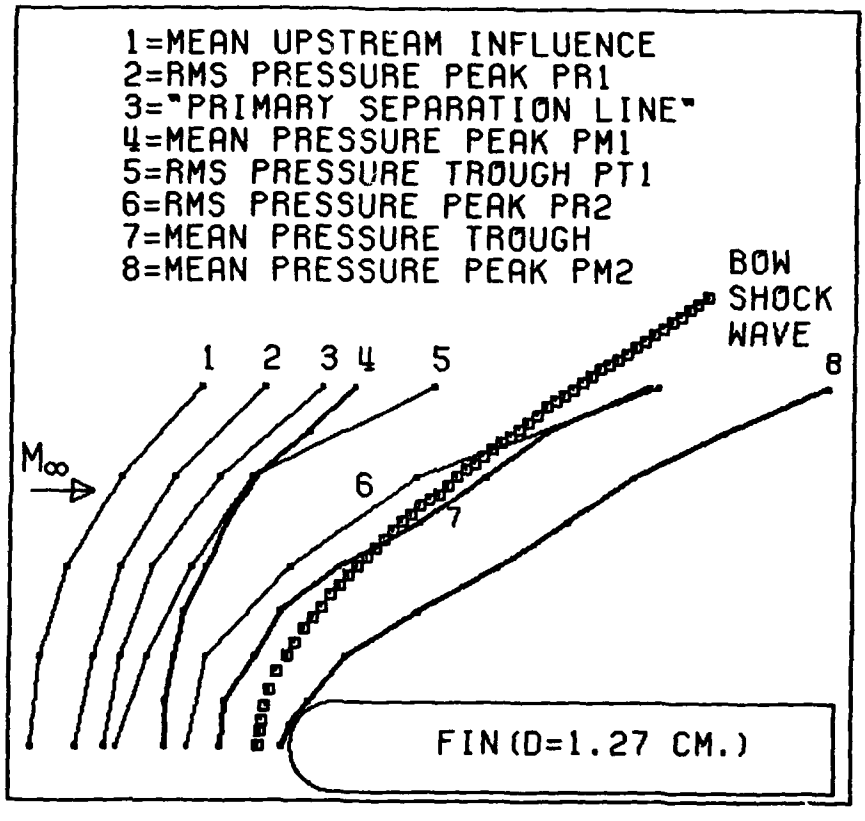

Figure 11. Locations of Characteristic Features of the R.M.S. and Mean Pressure Distributions and Surface Flow Pattern.

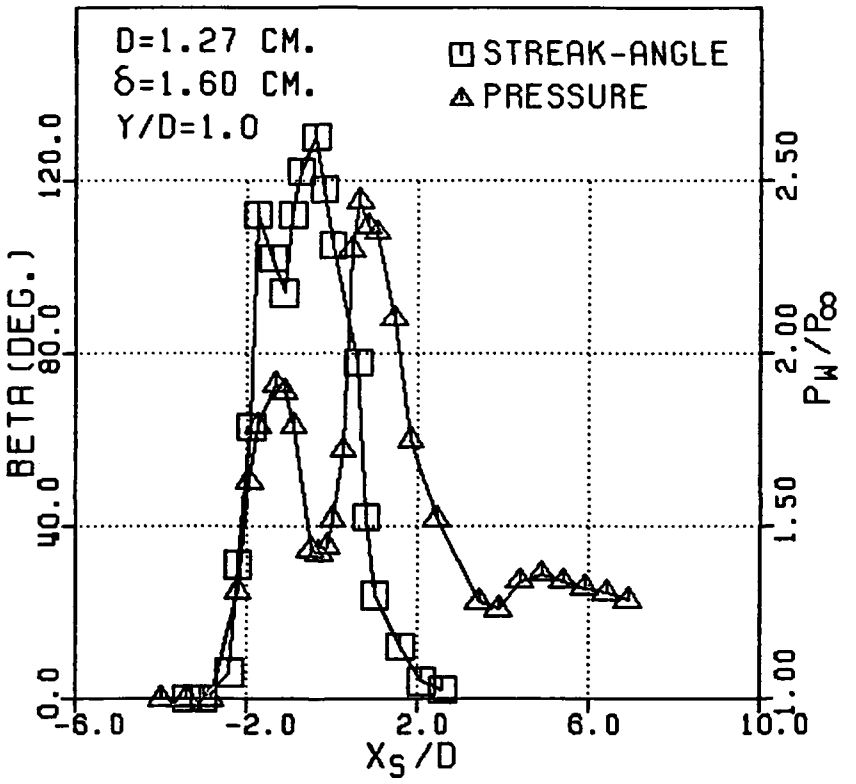

Figure 12. Surface Streak Angles and Mean Pressure Distribution at Y/D = 1.0.

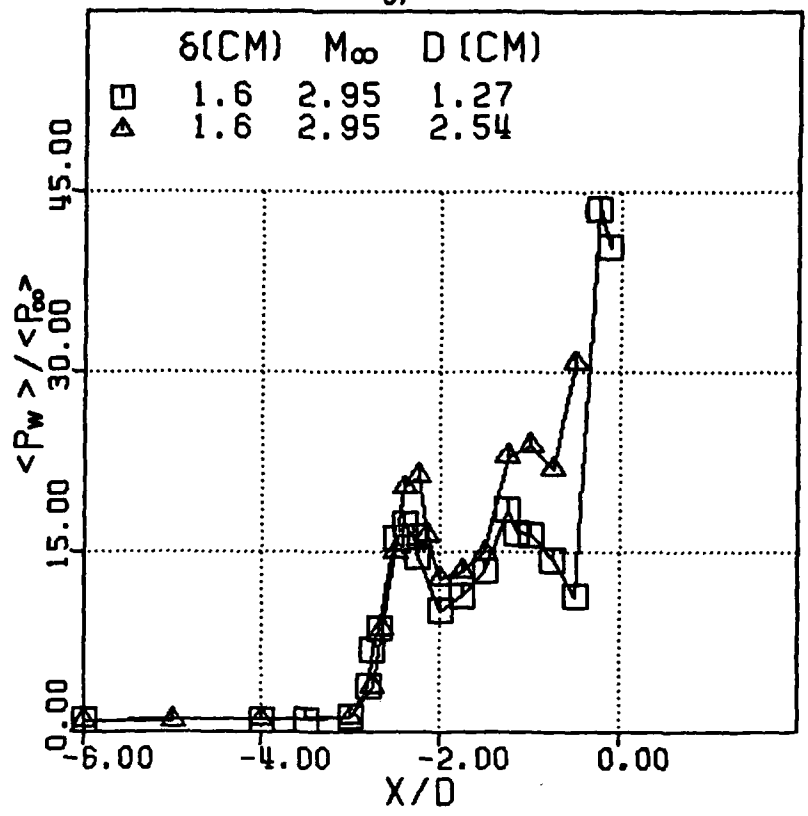

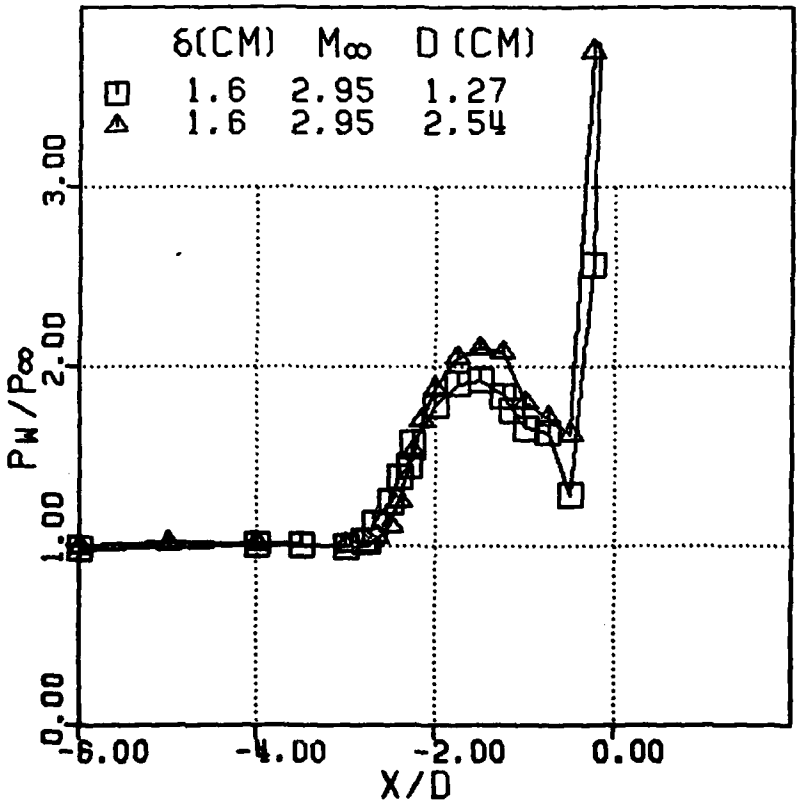

Figure 13. Effects of Diameter on Mean and R.M.S. Pressure Distributions on Centerline.

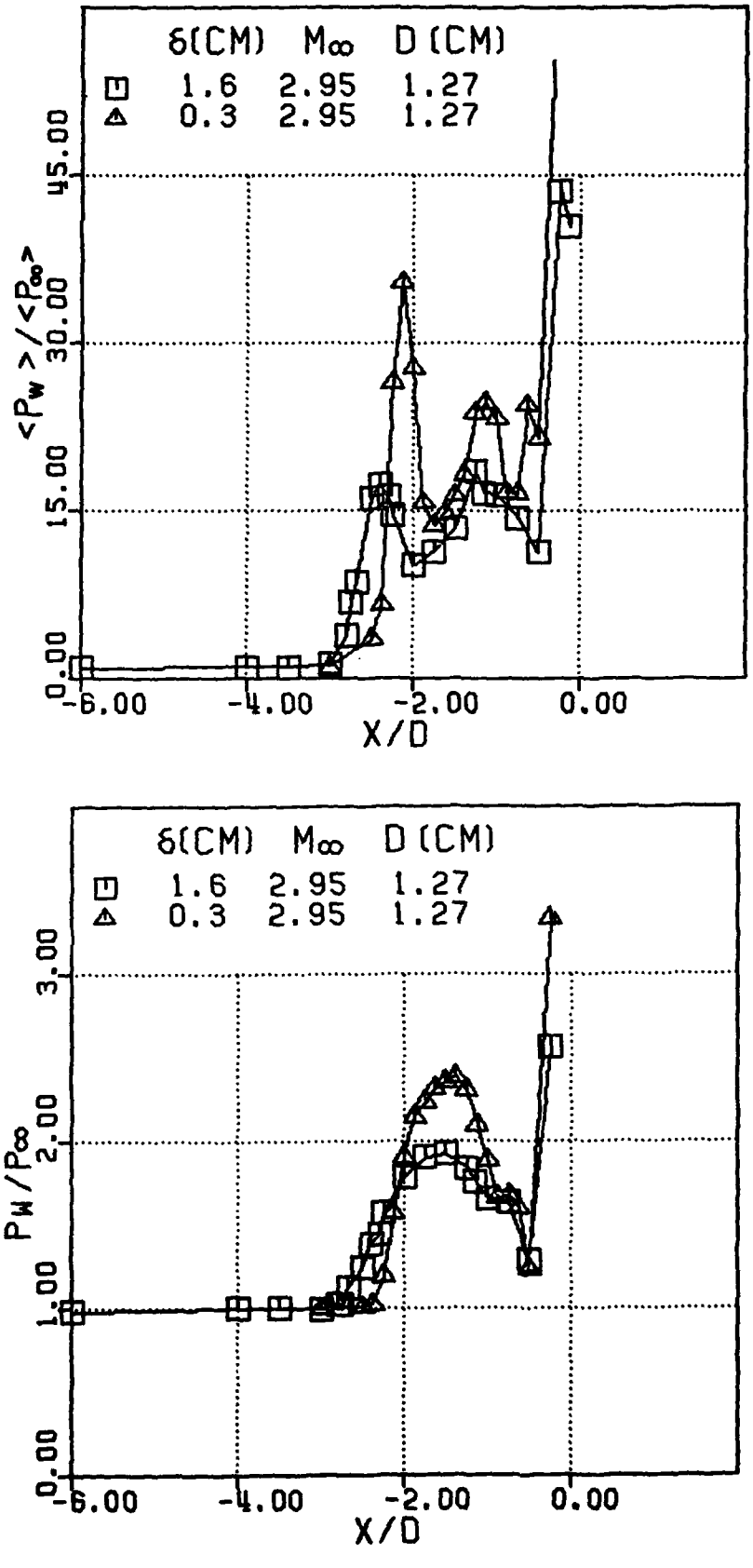

Figure 14. Effects of Boundary Layer Thickness on Mean and R.M.S. Pressure Distributions on Centerline.